Transpirative cooling potential of vegetation in urban environment using coupled CFD and leaf energy balance model

Lento Manickathan[1,2,*], Thijs Defraeye[1,2], Jonas Allegrini[1,2], Dominique Derome[2], Jan Carmeliet[1,2]
[1]Chair of Building Physics, ETH Zurich, Zurich, Switzerland
[2]Multiscale Studies in Building Physics, Empa, Dübendorf, Switzerland

Abstract

Urban greening strategies are increasingly being employed to provide natural cooling in cities and to mitigate the Urban Heat Island effect (UHI). In this study, we investigate the influence of environmental factors such as wind speed, relative humidity and solar radiation on cooling potential of a tree. Furthermore, we investigate the influence of tree height on the microclimate. A parametric study is performed using a coupled CFD and vegetation model, where the tree is modeled as a porous medium. The aim of the study is to determine how these parameters influence the capacity of vegetation to cool its environment. The study shows that the tree provides maximum cooling at low wind speed, low humidity, low radiation level and large tree height.

Introduction

Vegetation in the urban environment is increasingly being utilized to mitigate the Urban Heat Island (UHI) which is growing due to increasing urbanization. Trees in cities improve thermal comfort as they provide shading below the crown. Moreover, they extract heat from the air through the phase change of liquid water to water vapor, which occurs at the leaves (Defraeye et al., 2013). Typically, urban microclimate models employ a simplified empirical parameterization to represent vegetation. The estimation of cooling potential of vegetation using such models can make that some physical phenomena are not fully captured, such as the spatially varying cooling performance of vegetation.

The interaction between vegetation and the environment is a multi-physical phenomenon. Vegetation exchanges momentum, heat and mass with the air. The heat and mass exchanges can be modeled using various approaches of varying levels of complexities and accuracies. The big-leaf approach treats vegetation as one bulk leaf (Penman and Schofield, 1951; Shuttleworth and Wallace, 1985; Sellers et al., 1996), a dual-leaf model differentiates the sunlight from the sun-shaded leaf side (Dai et al., 2004) and a multi-layer canopy model can improve the vertical heterogeneity (Dolman, 1993; Krayenhoff et al., 2014; Leuning et al., 1995; Ryder et al., 2014; Wang and Jarvis, 1990). A computational fluid dynamics (CFD) approach (Hiraoka, 2005; Liang et al., 2006) was also used to solve the interaction between vegetation and environment, and provides a better understanding of the spatial (vertical and horizontal) variations in the temperature change due to vegetation. Such approaches have been used to study the influence of vegetation in urban areas (Bruse and Fleer, 1998; Gromke et al., 2014; Robitu et al., 2006). However, to the authors' knowledge, few studies have been performed to investigate the cooling performance of a tree, such as the study by Hiraoka (2005). Furthermore, a rigorous study on the influence of environmental properties such as wind speed, relative humidity and radiation on the performance of a tree and the resulting environmental cooling is lacking.

In this study, we investigate the transpirative cooling potential of a tree on the environment using a coupled airflow and vegetation model. The leaf temperature is assumed to be above the dew point and therefore the evaporation of the droplets from the leaf surface is not considered. The model implemented in the present study can eventually be extended for an arbitrary number of trees to study the influence of vegetation in cities. Furthermore, the present model can also be extended to study the water cycle through the plant and the soil, which is driven by the transpirative process. This is important as the transpiration rate through the stomata is directly linked to the water availability at the roots. Furthermore, the proposed method can help us to understand the response of vegetation during extreme environmental conditions such as drought and provides a more accurate prediction of the cooling performance.

Materials and methods

Mathematical formulation

The flow around and through vegetation is modeled using a computational fluid dynamics (CFD) approach where vegetation is modeled as a porous medium. Source terms in the CFD model are used to quantify the mass, momentum and energy exchanges with vegetation. The vegetation model, which consists of the leaf energy balance model, is solved together with the airflow to determine the heat and mass fluxes.

Flow of moist air

The turbulent flow of moist air around and through vegetation is modeled using incompressible Reynolds-Averaged Navier-Stokes (RANS) equations with a realizable $k-\varepsilon$ turbulence closure model. The conservation equations are (Hiraoka, 2005; Robitu et al., 2006; Bruse and Fleer, 1998; Kenjereš and Ter Kuile, 2013):

$$\nabla \cdot \overline{\boldsymbol{u}} = \frac{1}{\rho} S_\rho \tag{1}$$

$$\begin{aligned}\frac{\partial \overline{\boldsymbol{u}}}{\partial t} + \overline{\boldsymbol{u}} \cdot \nabla \overline{\boldsymbol{u}} = &-\frac{1}{\rho}\nabla \overline{P} + (\nu + \nu_t)\nabla^2 \overline{\boldsymbol{u}} \\ &- \boldsymbol{g}\beta\left(\overline{T} - T_0\right) - \frac{2}{3}\nabla k + \frac{1}{\rho}\boldsymbol{S}_u\end{aligned} \tag{2}$$

$$\frac{\partial \overline{T}}{\partial t} + \overline{\boldsymbol{u}} \cdot \nabla \overline{T} = \left(\frac{\nu}{\mathrm{Pr}} + \frac{\nu_t}{\mathrm{Pr_t}}\right)\nabla^2 \overline{T} + \frac{1}{\rho c_p} S_T \tag{3}$$

$$\frac{\partial \overline{q}}{\partial t} + \overline{\boldsymbol{u}} \cdot \nabla \overline{q} = \left(\frac{\nu}{\sigma_\nu} + \frac{\nu_t}{\sigma_{\nu_t}}\right)\nabla^2 \overline{q} + S_q \tag{4}$$

$$\frac{\partial k}{\partial t} + \overline{\boldsymbol{u}} \cdot \nabla k = \left(\nu + \frac{\nu_t}{\sigma_k}\right)\nabla^2 k + P_k - \varepsilon + \frac{1}{\rho} S_k \tag{5}$$

$$\begin{aligned}\frac{\partial \varepsilon}{\partial t} + \overline{\boldsymbol{u}} \cdot \nabla \varepsilon = &\left(\nu + \frac{\nu_t}{\sigma_\varepsilon}\right)\nabla^2 \varepsilon + C_{1\varepsilon} P_k \frac{\varepsilon}{k} \\ &- C_{2\varepsilon}\frac{\varepsilon^2}{k + \sqrt{\nu\varepsilon}} + \frac{1}{\rho} S_\varepsilon\end{aligned} \tag{6}$$

where $\overline{\boldsymbol{u}}$ [m s^{-1}] is the velocity vector, $\overline{P}$ [Pa] the hydrostatic pressure, $\overline{T}$ [K] the air temperature, $\overline{q}$ [kg kg^{-1}] the specific humidity, k [m^2 s^{-2}] the turbulent kinetic energy (TKE) and ε [m^2 s^{-3}] the TKE dissipation rate (TDR). The production of TKE is defined as $P_k = 2\nu_t|\mathbf{S}|^2$ [m^2 s^{-3}], where $\mathbf{S} = 1/2\ [\nabla\overline{\boldsymbol{u}} + (\nabla\overline{\boldsymbol{u}})^T]$ [s^{-1}] is the mean strain rate tensor. The environmental constants are density of air $\rho = 1.225$ kg m^{-3}, kinematic viscosity $\nu = 1.45 \times 10^{-5}$ m^2 s^{-1}, gravitational acceleration $\boldsymbol{g} = (0, 0, -9.81)$ m s^{-2}, the thermal expansion coefficient $\beta = 3 \times 10^{-3}$ and the specific heat capacity of air $c_p = 1003.5$ J kg^{-1} K^{-1}. The Prandtl number, the Schmidt number, the turbulent Prandtl and the turbulent Schmidt number are $\mathrm{Pr} = 0.9$, $\sigma = 0.9$, $\mathrm{Pr}_t = 0.7$ and $\sigma_t = 0.7$, respectively. The source terms are described in the following section.

Source terms for vegetation

Vegetation is discretized into finite volumes where the total amount of leaves per given volume is defined by the leaf area density (LAD), the total one-sided surface area of the leaf per given volume. The heat and mass exchanges between vegetation and air are solved in each of these finite volumes and provide the source terms in the air flow model. The source of mass S_ρ [kg m^{-3} s^{-1}] is:

$$S_\rho = \mathrm{LAD} \cdot E \tag{7}$$

where E [kg m^{-2} s^{-1}] is transpiration of water vapor from vegetation (Hiraoka, 2005). The source of momentum S_u [N m^{-3}] is:

$$S_u = -\rho c_d \mathrm{LAD}\,|\overline{\boldsymbol{u}}|\,\overline{\boldsymbol{u}} \tag{8}$$

where $c_d = 0.2$ is the leaf drag coefficient (Wilson and Shaw, 1977). The Reynolds number is assumed to be high enough to neglect the viscous drag of the leaves (Judd et al., 1996; Li et al., 1990; Liu et al., 1996). Furthermore, the momentum change of the flow due to transpiration is assumed to be negligible in comparison to the body forces exerted by vegetation. Therefore, a divergence-free constraint is enforced on the velocity-pressure coupling (Hiraoka, 2005). The source terms, S_k [W m^{-3}] and S_ε [W m^{-3} s^{-1}], are:

$$S_k = \rho C_d \mathrm{LAD}\left(\beta_p|\overline{\boldsymbol{u}}|^3 - \beta_d\,|\overline{\boldsymbol{u}}|\,k\right) \tag{9}$$

$$S_\varepsilon = \rho C_d \mathrm{LAD}\left(C_{4\varepsilon}\beta_p|\overline{\boldsymbol{u}}|^3\frac{\varepsilon}{k} - C_{5\varepsilon}\beta_d\,|\overline{\boldsymbol{u}}|\,\varepsilon\right) \tag{10}$$

where $\beta_p = 1.0$, $\beta_d = 5.1$, $C_{4\varepsilon} = 0.9$ and $C_{5\varepsilon} = 0.9$ (Katul et al., 2004; Sanz, 2003; Kenjereš and Ter Kuile, 2013). The source of temperature S_T [W m^{-3}] due to heat exchange is:

$$S_T = \mathrm{LAD} \cdot Q_s \tag{11}$$

where Q_s [W m^{-2}] is the sensible heat flux from vegetation into the air. The source of specific humidity S_q [kg kg^{-1} s^{-1}] into the flow is:

$$S_q = LAD \cdot E/\rho \tag{12}$$

Leaf energy balance

To determine the heat and mass fluxes between vegetation and air, a leaf energy balance is used. The leaf energy balance solves for a steady-state condition at which the exchanges between vegetation and air have reached an equilibrium rate (Boulard et al., 2008; Bruse and Fleer, 1998; Dauzat et al., 2001; Hiraoka, 2005):

$$R_n = \mathrm{LAD} \cdot (\lambda E + Q_s) \tag{13}$$

where R_n [W m^{-3}] is the net absorbed radiative heat flux density and $\lambda E \equiv Q_l$ [W m^{-2}] is the latent heat flux with a latent heat of vaporization of $\lambda = 2500$ kJ kg^{-1}. The net absorbed radiation is modeled using a semi-empirical approach and is defined as:

$$R_n = R_{sw,n} + R_{lw,n} \tag{14}$$

where $R_{sw,n}$ [W m^{-3}] is the net absorbed short-wave radiation and $R_{lw,n}$ [W m^{-3}] is the net absorbed long-wave radiation (Kichah et al., 2012). The net absorbed short-wave radiation is:

$$R_{sw,n} = \nabla \cdot R_{sw} = \frac{R_{sw}(z_2) - R_{sw}(z_1)}{\mathrm{d}z} \tag{15}$$

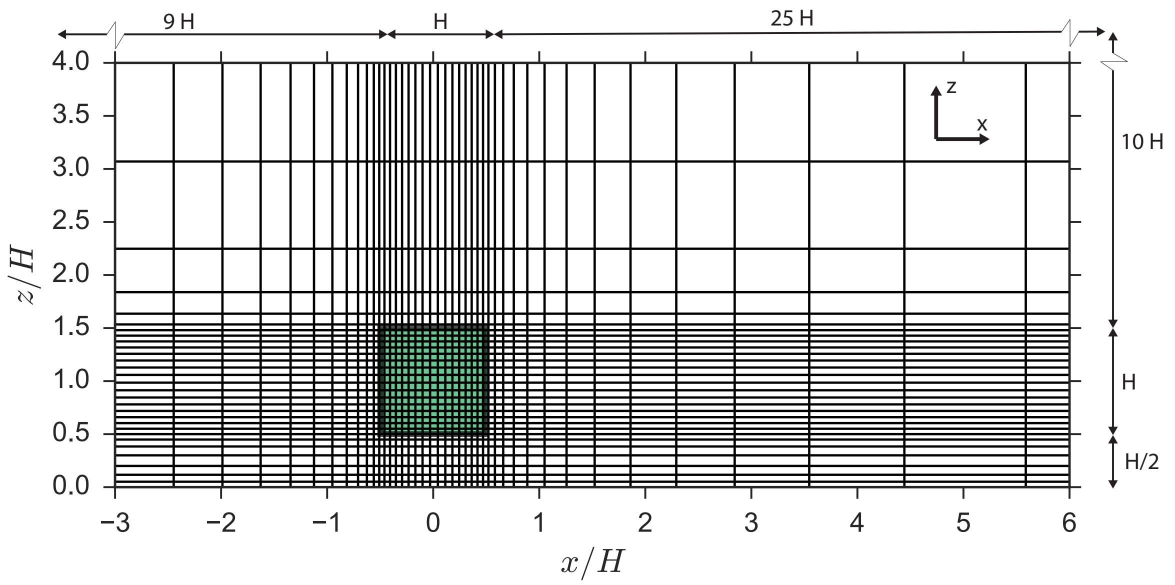

Figure 1: Simulation domain at the vicinity of the porous vegetation (green) with $H = 1$ m and, showing every 5^{th} cell nodes of the mesh.

where R_{sw} [$\mathrm{W\,m^{-2}}$] is the short-wave radiation at a given height z:

$$R_{sw,n} = R_{sw,0} \exp\left\{-k \int_{0\leq z\leq H}^{H} \mathrm{LAD}\ \mathrm{d}z\right\} \quad (16)$$

where $R_{sw,0}$ [$\mathrm{W\,m^{-2}}$] is the above-canopy short-wave radiative heat flux, assuming a sun at 90° altitude at noon and $k = 0.78$ is the short-wave radiation extinction coefficient (Kichah et al., 2012; Baille et al., 2006). The short-wave radiation is assumed to be varying only in the vertical direction. The net absorbed long-wave radiation is:

$$R_{lw,n} = C_{lw} \frac{R_{lw}}{H} \quad (17)$$

where $C_{lw} = 0.04$, the ratio of downward long-wave radiation and upward long-radiation at the top of vegetation, $R_{lw} = 350\ \mathrm{W\,m^{-2}}$, the above-canopy downward long-wave radiation for a sky temperature $T_{sky} = 15$ °C and $H = 1$ m, the height of the canopy. The sensible heat flux is defined as:

$$Q_s = 2\rho c_p \frac{T_l - T}{r_a} \quad (18)$$

where T_l [K] is the leaf surface temperature and r_a [$\mathrm{s\,m^{-1}}$] is the aerodynamic resistance (Dauzat et al., 2001; Robitu et al., 2006):

$$r_a = C \left(\frac{l}{|\overline{\boldsymbol{u}}|}\right)^{1/2} \quad (19)$$

where l [m] is the characteristic leaf size and $C = 130$ $\mathrm{s^{0.5}\,m^{-1}}$ is the proportionality factor (Dauzat et al., 2001). The latent heat flux is:

$$Q_l = \lambda \cdot \rho \frac{q_l - q}{r_a + r_s} \quad (20)$$

where q_l [$\mathrm{kg\,kg^{-1}}$] is the specific humidity at the surface of the leaf at the saturated vapor pressure condition with the leaf temperature of T_l. A constant stomatal resistance $r_s = 150\ \mathrm{s\,m^{-1}}$ is used in this study (Kichah et al., 2012). The energy balance (13), is satisfied by determining the leaf temperature:

$$T_l = T + \frac{r_a}{2\rho c_p}\left(\frac{R_n}{\mathrm{LAD}} - Q_l\right) \quad (21)$$

and requires an iterative procedure as Q_l is dependent on the leaf temperature.

Numerical model

The mathematical model of the coupled CFD and vegetation model is implemented into the OpenFOAM finite volume solver (Weller et al., 1998). The fluid domain is discretized into control volumes where the conservation equations and the leaf energy balances are solved together. The RANS equations are solved using a SIMPLE pressure-velocity coupling algorithm and a Boussinesq approximation is used to take into account the buoyancy force. The diffusive terms are discretized using second-order central differencing scheme and the convective terms are discretized using a second-order linear upwind scheme. The convergence criteria for residuals is ensured to be less than 10^{-8}, satisfying the conservation of heat flux in the domain. The numerical method is validated with real life experimental and numerical study of impatiens pot plants (jewelweed) in a greenhouse by Kichah et al. (2012).

Simulation domain

The simulation was performed in 2D, past a single square-shaped tree. The present mathematical model however can easily be extended to 3D with arbitrary number of trees (vegetation). Figure 1 shows the 2D

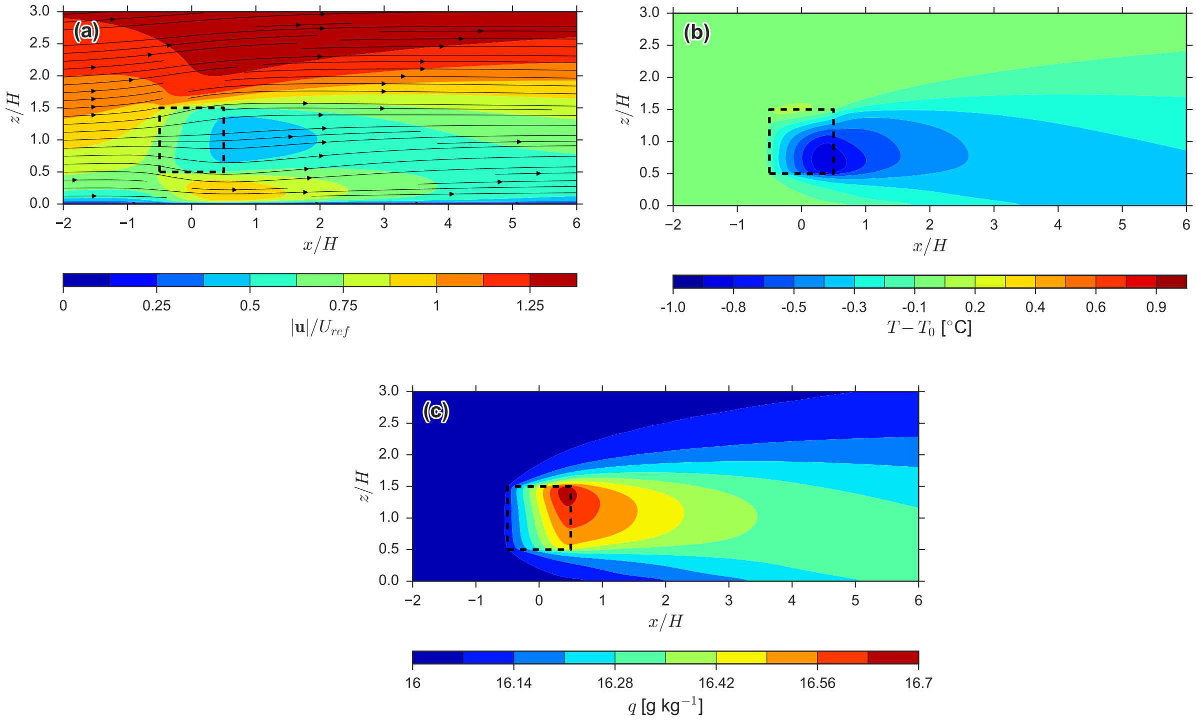

Figure 2: Influence of a single tree on the flow field: a) Normalized mean velocity norm $|\overline{\mathbf{u}}|/U_{ref}$, b) temperature change $T - T_0$ [°C] and c) specific humidity q $\left[g\ kg^{-1}\right]$. The inlet conditions are $U_{ref} = 1\ m\ s^{-1}$, $T_0 = 30$ °C, $RH = 60\%$ and $R_{sw} = 800\ W\ m^{-2}$. The dashed outline indicates the region containing the tree foliage.

simulation domain with a 1×1 m^2 tree of a height $H = 1$ m, with a leaf area density $LAD = 10$ m^2 m^{-3} and a leaf size $l = 0.1$ m.
The computational domain dimension and the numerical scheme are chosen based on urban physics best practice (Blocken, 2015; Franke et al., 2007; Tominaga et al., 2008). Additionally, a grid sensitivity analysis was performed to determine the required mesh resolution of 40 000 cells (Figure 1) with a cell-to-cell expansion ratio from the boundary of the porous region to the outflow, inlet, ground and top boundaries of 1.05, 1.05, 1.05 and 1.15, respectively.

Boundary conditions

The vegetation is immersed into an atmospheric boundary layer (ABL) (Richards and Hoxey, 1993):

$$\overline{u}\left(z\right) = \frac{u_*}{\kappa}\ln\left(\frac{z+z_0}{z_0}\right) \tag{22}$$

$$k\left(z\right) = \frac{u_*^2}{\sqrt{C_\mu}} \tag{23}$$

$$\varepsilon\left(z\right) = \frac{u_*^3}{\kappa\left(z+z_0\right)} \tag{24}$$

where u_* [m s^{-1}] is the friction velocity with $U_{ref} = 1$ m s^{-1} at $H_{ref} = 1$ m ($U_{10} = 1.593$ m s^{-1}), $\kappa = 0.41$, $C_\mu = 0.09$ and $z_0 = 0.0217$ m. Additionally, the inlet conditions are prescribed as $\overline{T}\left(z\right) = T_0 = 30$ °C and $\overline{q}\left(z\right) = q_0$ at a relative humidity of RH = 60 %. A no-slip adiabatic wall boundary condition with standard wall function is used for the ground surface. The adiabatic wall removes the thermal influence of the ground when quantifying the cooling power of vegetation. A zero normal gradient is used for specific humidity. At the top of the domain, a symmetric boundary condition is used and all other variables with zero normal gradient boundary condition. The outlet of the domain is a pressure outlet with zero static pressure and zero normal gradients for all other variables and assumes that the flow is fully developed.
The parametric study is performed by varying inlet boundary conditions and the vegetation size. The inlet conditions that are varied are the wind speed $U_{ref} = [0.1,\ 0.25,\ 0.5,\ 0.75,\ 1,\ 2,\ 3,\ 5]$ m s^{-1}, the relative humidity $RH = [20,\ 30,\ 40,\ 50,\ 60,\ 70,\ 80,\ 90,\ 95]$ % and the solar radiation $R_{sw} = [100,\ 400,\ 800,\ 1000]$ W m^{-2}. The tree height is varied as $\tilde{H} = [1H,\ 2H,\ 3H,\ 5H]$ m. These parameters are chosen as they are assumed to have the largest impact on the cooling performance of vegetation.

Results and discussion

The impact of vegetation on the urban microclimate is studied firstly by investigating the change in flow field. Thereafter, the influence of the wind speed, relative humidity, solar radiation and tree height on the cooling performance is investigated.

Flow field

The influence of a tree on the flow is determined by investigating the velocity, temperature and humidity. Figure 2 shows the normalized mean velocity norm

$|\boldsymbol{u}|/U_{ref}$, the air temperature change $T - T_0$ [°C] and the humidity ratio q [$\mathrm{g\,kg^{-1}}$]. Note that the overbar is omitted for convenience. The velocity field shows that the vegetation reduces the wake velocity to more than half the inlet velocity. In addition, the transpirative cooling reduces the air temperature by nearly 1 °C and increases the humidity ratio by 0.7 $\mathrm{g\,kg^{-1}}$. The maximum reduction in temperature occurs at the bottom of the foliage whereas the maximum humidity rise occurs at the top of the vegetation. However, we also observe that there is slight increase in the air temperature at the top of the tree ($z/H = 1.5$) as the temperature rises above 30 °C. This is because the canopy is directly exposed to solar radiation which results in an increased leaf temperature. As a result, there is a rise in air temperature at the top of vegetation.

Parametric study

The parametric study is performed by varying the wind speed, relative humidity, solar radiation and tree height independently and keeping all other variables constant. The response to these variations gives insight on their influence and, furthermore, enables an accurate prediction of the cooling potential of vegetation.

Influence of wind speed

The influence of wind speed on the cooling provided by the tree is studied by investigating the change in air temperature $T - T_0$ [°C] behind the vegetation. The vertical profile is sampled at $x/H = 1.5$ ($1H$ m behind the tree) from $z/H = 0$ to $z/H = 4$ for various wind speeds (Figure 3).

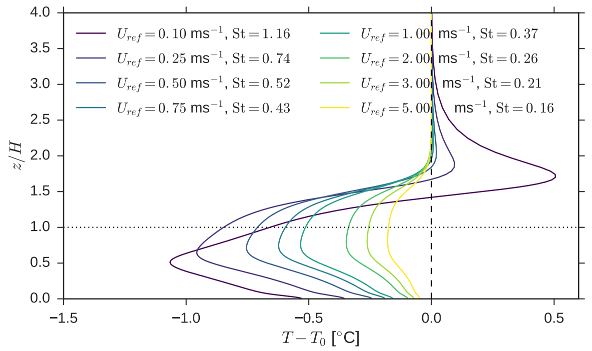

Figure 3: Influence of wind speed U_{ref} $\left[m\ s^{-1}\right]$ on the air temperature change $T - T_0$ $\left[°C\right]$ for vertical profiles extracted behind the tree at $x/H = 1.5$.

Figure 3 shows that the cooling occurs predominantly at lower heights ($z/H < 1.5$), near the tree foliage. At higher heights, we see that in some cases the air temperature rises above the inlet temperature. This is because the top of vegetation is directly exposed to solar radiation which results in a high leaf temperature and thereby results in an increase of air temperature (Figure 2b).

Furthermore, Figure 3 shows that the maximum cooling is observed at the lowest wind speed ($U_{ref} = 0.1$ $\mathrm{m\,s^{-1}}$) at $z/H \approx 0.5$. However, simultaneously the maximum rise in air temperature is also observed, at $z/H \approx 1.75$. This occurs because the heat extracted from the air with respect to the total enthalpy convected through the domain is higher for lower velocity. The Stanton number measures this ratio of heat transferred into the fluid to the total enthalpy of the air that is convected:

$$\mathrm{St} = \frac{h}{\dot{m} c_p} = \frac{h}{\rho u c_p} \tag{25}$$

where h [$\mathrm{W\,m^{-2}\,K^{-1}}$] is the average convective heat transfer coefficient of the leaves and $\dot{m}$ [$\mathrm{kg\,s^{-1}\,m^{-2}}$] is the mass flux in the domain. Substituting (18) and (19) into Stanton number (25) gives:

$$\mathrm{St} = \frac{2}{C\ l^{1/2}} \left(\frac{1}{u}\right)^{1/2} \tag{26}$$

and we see that the Stanton number is simply proportional to the inverse root of the wind speed. The Stanton number is $\mathrm{St} = 1.16$ at $U_{ref} = 0.1$ and $\mathrm{St} = 0.16$ at $U_{ref} = 5$ m (Figure 3). Thus, a low wind speed results in a larger change in air temperature.

Influence of relative humidity

Figure 4 shows the influence of relative humidity RH on the air temperature. It is clear that maximum cooling provided by the vegetation occurs at low RH, with peak temperature drop of $T - T_0 \approx -1.4$ °C at RH = 20 %. Above RH = 80 %, the air temperature change is overall positive.

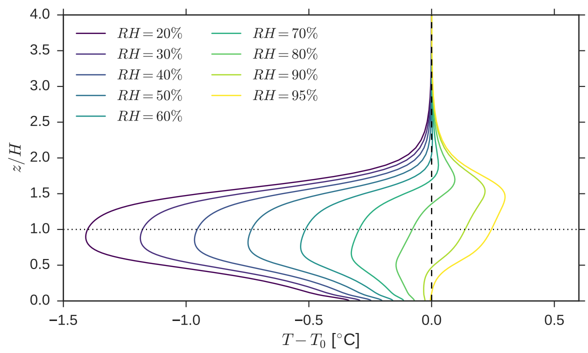

Figure 4: Influence of relative humidity RH [%] on the air temperature change $T - T_0$ $\left[°C\right]$ for vertical profiles extracted behind the tree at $x/H = 1.5$.

This study clarifies the influence of transpiration on the cooling provided by vegetation. A low RH results in a higher transpiration from vegetation as vapor quantity in the air is lower (assuming the influence of air temperature change is small). At low RH, a low humidity in air results in a higher latent heat flux (20) and causes the observed peak cooling. At high RH, the transpiration is small and causes the rise in air temperature. However, one must note that the thermal benefit provided by the shading of the tree on the building facade and ground is not modeled in this study. In such real scenario, the presence of vegetation will provide a consistent cooling regardless of the moisture content of air due to other cooling effects of shading on the environment.

Influence of solar radiation

Figure 5 shows the influence of solar radiation R_{sw} on the air temperature. The figure shows that cooling provided by the tree is highest when radiation level is low, since more heat needs to be extracted from the airflow for evaporation. At higher solar radiation, the cooling is reduced with a slight increase in air temperature above the tree canopy ($z/H \approx 2$). This is due to the high absorption of solar radiation at the top of the tree resulting in the higher leaf temperature. The stomatal response of the solar radiation was not modeled in the present study. In such cases, the influence of solar radiation on the cooling could be non-linear. Therefore, further studies must be performed on the coupled behavior of stomatal resistance and environmental conditions.

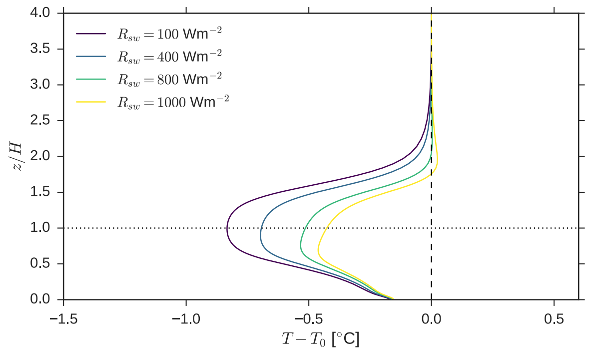

Figure 5: Influence of short-wave radiative heat flux R_{sw} $[W\ m^{-2}]$ on the air temperature change $T - T_0$ $[°C]$ for vertical profiles extracted behind the tree at $x/H = 1.5$.

Influence of tree height

The final parametric study is performed on understanding the influence of tree height $\tilde{H} = n \cdot H$. Figure 6 shows the influence of tree height on air temperature. The figure shows that, with increasing tree height, a larger volume of air is cooled. Furthermore, the maximum air temperature drop increases from -0.5 to -1.0 °C when increasing the tree height $\tilde{H} = 1$ m to $\tilde{H} = 5$ m. However, it cannot be concluded yet that increasing the tree height increases the cooling performance of the tree, as the total quantity of leaves in the domain, $\int$ LAD dV [m^2] increases as well. To determine the cooling potential of vegetation independently of the amount of leaves in the domain, we can study the ratio of total sensible heat flux to the total leaf area in the domain, denoted as $\tilde{Q}_s$ [W m^{-2}]:

$$\tilde{Q}_s \equiv \frac{\int LAD \cdot Q_s \,\mathrm{d}V}{\int LAD \,\mathrm{d}V} \tag{27}$$

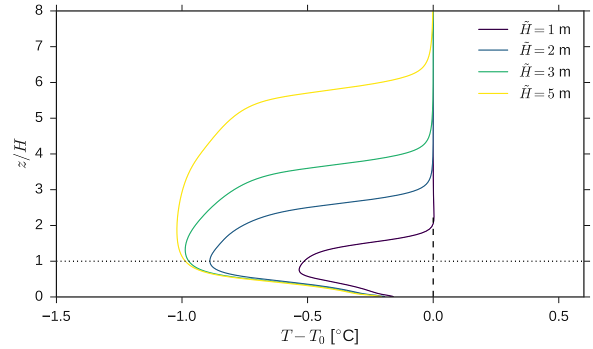

Figure 6: Influence of tree height $\tilde{H} = n \cdot H$ $[m]$ on the air temperature change $T - T_0$ $[°C]$ for vertical profiles extracted behind the tree at $x/H = 1.5$.

The influence of tree height on the normalized sensible heat flux $\tilde{Q}_s$ is shown in Figure 7. The figure shows conclusively that it is beneficial to increase the tree height as $\tilde{Q}_s$ increases with the tree height $\tilde{H}$. Therefore, trees with a high vegetation canopy can provide substantial improvement to the urban microclimate compared to lower trees. However, this relationship is also apparent that it has a decaying growth and eventually may not provide additional cooling performance.

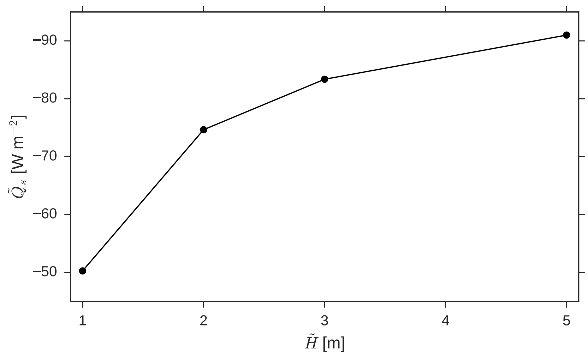

Figure 7: Influence of tree height $\tilde{H} = n \cdot H$ $[m]$ on the normalized sensible heat flux $\tilde{Q}_s$ $[W\ m^{-2}]$.

Conclusion

The proposed numerical modeling approach captures the flows through the tree foliage. The model is used to increase our understanding of the role of transpiration of vegetation in urban environments and to assess its resulting cooling potential. In conclusion, the study on the influence of wind speed, relative humidity, solar radiation and tree height shows that:

- At lower wind speeds, vegetation provides a higher cooling rate. The Stanton number is inversely proportional to wind speed.
- The transpirative cooling is larger in arid conditions.
- High solar radiation reduces the cooling provided by vegetation.
- Tree height is a dominant factor when determining the cooling performance of vegetation.

- Taller trees are more effective in providing cooling than shorter trees.

Acknowledgement

The project is funded by the Chair of Building Physics, ETHZ.

References

Baille, A., R. P. Gutierrez Colomer, and M. M. Gonzalez-Real (2006). Analysis of intercepted radiation and dry matter accumulation in rose flower shoots. *Agricultural and Forest Meteorology 137*(1-2), 68–80.

Blocken, B. (2015). Computational Fluid Dynamics for urban physics: Importance, scales, possibilities, limitations and ten tips and tricks towards accurate and reliable simulations. *Building and Environment 91*, 219–245.

Boulard, T., H. Fatnassi, H. Majdoubi, and L. Bouirden (2008). Airflow and microclimate patterns in a one-hectare canary type greenhouse: An experimental and CFD assisted study. *Acta Horticulturae 801 PART 2*, 837–845.

Bruse, M. and H. Fleer (1998). Simulating surface-plant-air interactions inside urban environments with a three dimensional numerical model. *Environmental Modelling & Software 13*(3-4), 373–384.

Dai, Y., R. E. Dickinson, and Y.-P. Wang (2004). A Two-Big-Leaf model for canopy temperature, photosynthesis, and stomatal conductance. *Journal of Climate 17*(12), 2281–2299.

Dauzat, J., B. Rapidel, and A. Berger (2001). Simulation of leaf transpiration and sap flow in virtual plants: model description and application to a coffee plantation in Costa Rica. *Agricultural and Forest Meteorology 109*(2), 143–160.

Defraeye, T., P. Verboven, D. Derome, J. Carmeliet, and B. Nicolai (2013). Stomatal transpiration and droplet evaporation on leaf surfaces by a microscale modelling approach. *International Journal of Heat and Mass Transfer 65*, 180–191.

Dolman, A. J. (1993). A multiple-source land surface energy balance model for use in general circulation models. *Agricultural and Forest Meteorology 65*(1-2), 21–45.

Franke, J., A. Hellsten, H. Schlunzen, and B. Carissimo (2007). *Best practice guideline for the CFD simulation of flows in the urban environment: COST action 732 quality assurance and improvement of microscale meteorological models.* Number July 2016.

Gromke, C., B. Blocken, W. Janssen, B. Merema, T. van Hooff, and H. Timmermans (2014). CFD analysis of transpirational cooling by vegetation: Case study for specific meteorological conditions during a heat wave in Arnhem, Netherlands. *Building and Environment 83*, 11–26.

Hiraoka, H. (2005). An investigation of the effect of environmental factors on the budgets of heat, water vapor, and carbon dioxide within a tree. *Energy 30*(2-4 SPEC. ISS.), 281–298.

Judd, M., M. Raupach, and J. Finnigan (1996). A wind tunnel study of turbulent flow around single and multiple windbreaks, part I: velocity fields. *Boundary-Layer Meteorology* (1974), 127–165.

Katul, G. G., L. Mahrt, D. Poggi, and C. Sanz (2004). One- and two-equation models for canopy turbulence. *Boundary-Layer Meteorology 113*(1), 81–109.

Kenjereš, S. and B. Ter Kuile (2013). Modelling and simulations of turbulent flows in urban areas with vegetation. *Journal of Wind Engineering and Industrial Aerodynamics 123*(PA), 43–55.

Kichah, A., P.-e. Bournet, C. Migeon, T. Boulard, and S. Antipolis (2012). Measurement and CFD simulation of microclimate characteristics and transpiration of an Impatiens pot plant crop in a greenhouse. *Biosystems Engineering 112*(1), 22–34.

Krayenhoff, E. S., A. Christen, A. Martilli, and T. R. Oke (2014). A Multi-layer Radiation Model for Urban Neighbourhoods with Trees. *Boundary-Layer Meteorology 151*(1), 139–178.

Leuning, R., F. M. Kelliher, D. G. G. de Pury, and E. D. Schulze (1995). Leaf nitrogen, photosynthesis, conductance and transpiration: Scaling from leaves to canopies. *Plant, Cell and Environment 18*(10), 1183–1200.

Li, Z., J. D. Lin, and D. R. Miller (1990). Air flow over and through a forest edge: A steady-state numerical simulation. *Boundary-Layer Meteorology 51*(1-2), 179–197.

Liang, L., L. Xiaofeng, L. Borong, and Z. Yingxin (2006). Improved k-ϵ two-equation turbulence model for canopy flow. *Atmospheric Environment 40*(4), 762–770.

Liu, J., J. M. Chen, T. a. Black, and M. D. Novak (1996). E-ϵ modelling of turbulent air flow downwind of a model forest edge. *Boundary-Layer Meteorology 77*(1), 21–44.

Penman, H. L. and R. K. Schofield (1951). Some physical aspects of assimilation and transpiration. *Carbon Dioxide Fixation and Photosynthesis 5.*

Richards, P. and R. Hoxey (1993). Appropriate boundary conditions for computational wind engineering models using the k-ϵ turbulence model. *Journal of Wind Engineering and Industrial Aerodynamics 46-47*, 145–153.

Robitu, M., M. Musy, C. Inard, and D. Groleau (2006, apr). Modeling the influence of vegetation and water pond on urban microclimate. *Solar Energy 80*(4), 435–447.

Ryder, J., J. Polcher, P. Peylin, C. Ottlé, Y. Chen, E. van Gorsel, V. Haverd, M. J. McGrath, K. Naudts, J. Otto, a. Valade, and S. Luyssaert (2014). A multi-layer land surface energy budget model for implicit coupling with global atmospheric simulations. *Geoscientific Model Development Discussions 7*(6), 8649–8701.

Sanz, C. (2003). A note on k-ϵ modeling of vegetation canopy air-flows. *Boundary-Layer Meteorology 108*(1992), 191–197.

Sellers, P. J., D. A. Randall, G. J. Collatz, J. A. Berry, C. B. Field, D. A. Dazlich, C. Zhang, G. D. Collelo, and L. Bounoua (1996). A revised land surface parameterization (SiB2) for atmospheric GCMs. Part I: Model formulation.

Shuttleworth, W. J. and J. S. Wallace (1985). Evaporation from sparse crops-an energy combination theory. *Quarterly Journal of the Royal Meteorological Society 111*(469), 839–855.

Tominaga, Y., A. Mochida, R. Yoshie, H. Kataoka, T. Nozu, M. Yoshikawa, and T. Shirasawa (2008). AIJ guidelines for practical applications of CFD to pedestrian wind environment around buildings. *Journal of Wind Engineering and Industrial Aerodynamics 96*(10-11), 1749–1761.

Wang, Y. P. and P. G. Jarvis (1990). Description and validation of an array model - MAESTRO. *Agricultural and Forest Meteorology 51*(3-4), 257–280.

Weller, H. G., G. Tabor, H. Jasak, and C. Fureby (1998). A tensorial approach to computational continuum mechanics using object-oriented techniques. *Computers in Physics 12*(6), 620.

Wilson, N. R. and R. H. Shaw (1977). A Higher Order Closure Model for Canopy Flow. *Journal of Applied Meteorology 16*(11), 1197–1205.